16.512, Rocket Propulsion
Prof. Manuel Martinez-Sanchez
Lecture 29: Rotordynamics Problems

1. Turbopump Rotor Dynamics

Because of high power density and low damping in rocket turbopumps, these machines exhibit in their most extreme form a variety of vibration effects, which are either absent or masked by normal damping mechanisms in other turbo machines. The low damping is especially prominent in liquid hydrogen pumps, because of the very low viscosity and density of this medium. Oil squeeze film dampers are precluded in any cryogenic medium.

The general frame work of Rotor Dynamics is now well established, through a combination of classical analysis and detailed numerical simulation [49, 50, 51]. Intensive efforts on the application of these theoretical methods to a specific rocket turbopump are described by Ek[52], and were instrumental in pointing the way to a series of improvements that resolved a serious development problem in the SSME. The greatest difficulty in this field remains the precise characterization of the fluid forces acting on the rotor at components such as seals, turbines, or impellers. Once these are specified, numerical models of great power and versatility can be brought to bear for analyzing the dynamics of a given configuration. Because of the remaining uncertainties in the basic forces. Ek's 1978 recommendation [52] remains valid today: "Prediction of stability in a new design must be viewed with skepticism. A prediction of instability should, however, be taken very seriously".

2. Forced and Self- Excited Vibrations

Three are two types of rotor dynamics problems:

(a) Resonances which usually occur when the rotating speed coincides with one of the natural ("critical") frequencies of the rotor (including its supporting structure). These fall in the category of Forced Vibrations, in which an excitation force produces deflection responses of an amplitude which increases as the excitation frequency approaches a critical frequency. If the excitation is at exact resonance, the amplitude grows linearly in time at first, and then, if viscous damping exists, it approaches a limit which is inversely proportional to the damping factor. Removal of the excitation removes the response. The exciting forces are typically related to rotor mass imbalance or geometrical imperfections. Resonances rarely pose serious problems, unless the steady operating point lies very close to one critical. On the other hand, since the structure is made as light as practical, many natural modes usually exist, several of them either below or not far above the operating range. Efforts are made in the design phase to create a relatively wide range of resonance- free speeds around the normal operating point. Passage through criticals, if made rapidly enough, is not a severe condition.

Table 3 (Ref [53]) shows the critical frequencies of the SSME fuel turbopump. Notice that several of the shaft modes are split into adjacent pairs of critical frequencies because of the lack of symmetry of the casing structural supports,

even though the bearing structure itself is symmetric. This asymmetry is in general a beneficial effect, and provides a sort of effective damping [54].

(b) Self- Excited Vibrations These are autonomous oscillations, in which the shaft vibrates at one of its natural frequencies (not equal to the shaft speed), and due to some positive feedback mechanism, absorbs energy from an external source (usually the fluid) into the vibrational mode. Exact balancing does not remove this type of vibration. Once initiated, if damping is insufficient, the vibration will increase exponentially in amplitude until some nonlinear mechanism intervenes, or until rubbing occurs. Self-excited vibrations are also called "rotor-dynamic instabilities" or "sub- synchronous vibrations". The latter designation is due to the fact that they are most often observed in the lowest shaft mode when the rotating speed is well above the frequency of this mode. For some mechanisms of excitation, the ratio of the rotation speed at onset of instability to the frequency of the vibration excited is a simple integer,

COUPLED HPFTP ROTOR AND CASE MODES

Mode	Frequency(Hz)	Description
1	-	Rotor free spin, X
2	47.0	Case rocking, Y
3	100.8	Case rocking, Z
4	196.4	Case rocking + bending, Y
5	197.5	Diffuser torsion
6	249.8	Case rocking + bending, Z
7	287.6	Rotor translation, Y
8	321.0[a]	Rotor translation, Z
9	375.1	Rotor rocking, Z
10	424.0[a]	Rotor rocking, Y
11	463.7	Rotor axial, X
12	488.7	Case + rotor rocking, Z
13	513.6	Rotor bending, Y
14	515.0[a]	Rotor bending, Z
15	554.8	Turbine case torsion, X
16	574.7	Diffuser bending, Y
17	577.4	Diffuser bending, Z
18	599.4	Case + rotor rocking, Y
19	650.4	Case torsion, X
20	657.3	Case axial, X
21	694.9	Turbine case bending, Z

or an excitation threshold Table 3 exists at an integer multiple of the excited frequency [55]. However, thus is not universally the case, and, in fact, no such simple ratio or threshold seems to exist for the most important mechanisms (seal or turbine blade-tip effects). It is true, however, that the rate of energy input into the vibration increases with power level of the turbopump, and hence with its speed; thus, the machine damping may be sufficient to compensate for this effect at low rotation speeds, but, as speed increases, a threshold will appear, beyond which the operation is unstable.

The two types of vibration described can be easily distinguished in tests by plotting a series of vibration spectra at increasing rotational speed (a cascade diagram, Fig. 1). Here

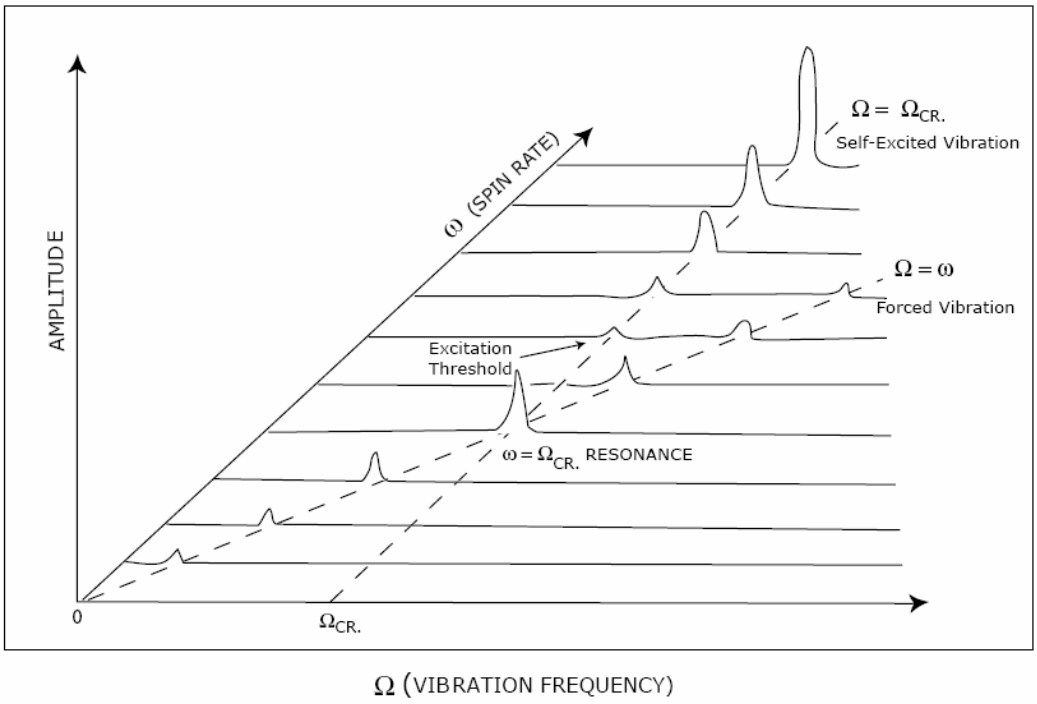

Fig. 1. A cascade diagram showing one mode only. Forced vibrations related to imbalance are seen at $\Omega = \omega$, with a resonance when $\omega = \Omega_{cr}$. Also shown is a sub-synchronous, self-excited vibration at $\Omega = \Omega_{cr}$.

ω is the shaft speed, Ω is the angular frequency of the vibration, and Ω_{cr} is the critical or natural frequency (only one shown). As indicated, no self-excited vibration is visible until ω reaches some threshold, and then the instability becomes more and more prominent. The amplitude itself depends on conditions when the spectrum is taken (variation rate of ω dwell time at the given condition, etc.), but the frequency information is still quite useful.

3. Sources of Rotor-Dynamic Excitation: Cross-Coupled Forces

The most important excitation mechanisms are related to the production of cross-forces when the shaft is offset from its central location. Before describing some specific examples, the generic dynamic effects of these cross-forces will be discussed.

Qualitatively, if a cross-force F_y results from a shaft offset e_x, this force exerts a torque $F_y e_x$ with respect to the nominal shaft center. It is well known that any linear vibration in the x-y plane can be resolved into a forward and a backward circular oscillations. Of these two, one (the forward component in Fig 2. is reinforced by the resulting torque $F_y e_x$, which, being produced by the displacement itself, will remain synchronized to it. This is the basic instability mechanism.

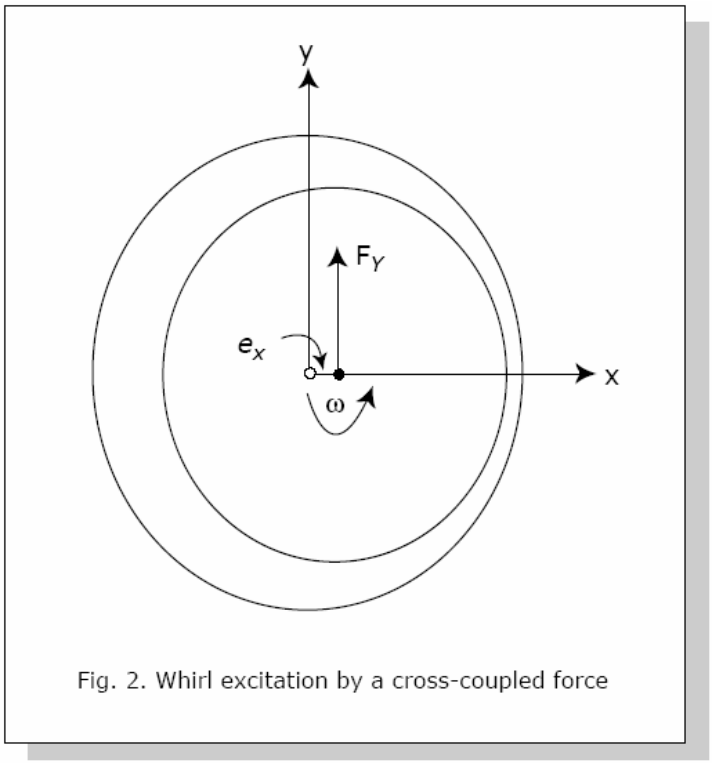

Fig. 2. Whirl excitation by a cross-coupled force

For a simple linearized analysis, suppose the fluid effects are such that a general transverse displacement (e_x, e_y) and displacement rate $\left(\dot{e}_x, \dot{e}_y\right)$ of the shaft produces forces (F_x, F_y) according to

$$\begin{Bmatrix} F_x \\ F_y \end{Bmatrix} = \begin{bmatrix} -K_{xx} & K_{xy} \\ -K_{xy} & -K_{xx} \end{bmatrix} \begin{Bmatrix} e_x \\ e_y \end{Bmatrix} + \begin{bmatrix} -C_{xx} & C_{xy} \\ -C_{xy} & -C_{xx} \end{bmatrix} \begin{Bmatrix} \dot{e}_x \\ \dot{e}_y \end{Bmatrix} \qquad (1)$$

The coefficients K_{xx} and K_{xy} are the direct and cross-coupled stiffness, respectively. Notice that the cylindrical symmetry has been exploited to reduce to <u>two</u> the number of stiffness factors, and that a positive K_{xx} is restoring, and will augment the <u>structural stiffness</u> K_0, although, in general, $|K_{xx}| << K_0$. Similar comments apply to the damping coefficients C_{xx}, C_{xy}, except that C_{xx} may be of the same order as any additional damping C_0.

Define a complex displacement

$$e_x + i\, e_y = z \tag{2}$$

then
$$\begin{cases} M\dfrac{d^2 e_x}{dt^2} = -(K_0 + K_{xx})\, e_x + K_{xy} e_y \quad -(C_0 + C_{xx})\,\dot{e}_x + C_{xy}\,\dot{e}_y \\ M\dfrac{d^2 e_y}{dt^2} = -K_{xy} e_x - (K_0 + K_{xx}) e_y - C_{yy}\,\dot{e}_x - (C_0 + C_{xx})\,\dot{e}_y \end{cases} \tag{3 a, b}$$

Add i x (3b) to (3a):

$$M\frac{d^2 z}{dt^2} = -(K_0 + K_{xx})\underbrace{(e_x + i e_y)}_{z} + K_{xy}\underbrace{(e_y - i e_x)}_{-i\,z} - - - -$$

$$M\frac{d^2 z}{dt^2} = -(\underbrace{K_0 + K_{xx} + i K_{xy}}_{K})z - (\underbrace{C_0 + C_{xx} + i\, C_{xy}}_{C})\,\dot{z}$$

$$\ddot{z} + \frac{C}{M}\dot{z} + \frac{K}{M} z = 0 \tag{4}$$

Put now $z = \hat{z}\, e^{i\Omega t}$ (unstable if $\Omega_I < 0$) $\Rightarrow$ $\quad + \Omega^2 - i\frac{C}{M}\Omega - \frac{K}{M} = 0$ (5)

$$\Omega = i\frac{C}{2M} \pm \sqrt{-\left(\frac{C}{2M}\right)^2 + \frac{K}{M}} \tag{6}$$

Call $K_{xx} = \dfrac{K_{xy}}{K_0}$ $\quad K_{yy} = \dfrac{K_{xy}}{K_0}$ $\quad \zeta = \dfrac{1}{2}\dfrac{C_0 + C_{xx}}{\sqrt{K_0 M}}$ $\quad \eta = \dfrac{1}{2}\dfrac{C_{xy}}{\sqrt{K_0 M}}$

$$\frac{\Omega}{\Omega_0} = \frac{\Omega}{\sqrt{\frac{K_0}{M}}} = \quad -i\frac{C_0 + C_{xx} + iC_{xy}}{2\sqrt{K_0 M}} \pm \sqrt{\left(\frac{C_0 + C_{xx} + iC_{xy}}{2\sqrt{K_0 M}}\right)^2 + \frac{K_0 + K_{xx} + iK_{xy}}{K_0}}$$

$$\frac{\Omega}{\sqrt{K_0/M}} = \quad = i(\zeta + i\eta) \pm \sqrt{(\zeta + i\eta)^2 + 1 + K_{xx} + iK_{xy}} \tag{7}$$

$$\gamma \quad \zeta \ll, \qquad \eta \ll 1, \quad K_{xy} \ll 1 \qquad \frac{\Omega}{\sqrt{K_0/M}} \simeq i\zeta - \eta \pm \left(1 + \frac{K_{xx}}{2} + i\frac{K_{xy}}{2}\right)$$

$$\frac{\Omega}{\Omega_0} = \begin{cases} + & 1 + \frac{K_{xx}}{2} - \eta + i\left(\zeta + \frac{1}{2}k_{xy}\right) \\ - & -1 - \frac{K_{xx}}{2} - \eta + i\left(\zeta - \frac{1}{2}k_{xy}\right) \end{cases} \tag{8}$$

For $K_{xy} > 0$, $\boxed{\text{if } \frac{1}{2}K_{xy} > \zeta, \quad \text{unstable}}$ (9)

$$\frac{K_{xy}}{K_0} > \frac{C_0 + C_{xx}}{\sqrt{K_0 M}} \qquad \boxed{K_{xy} > \Omega_0 (C_0 + C_{xx})} \text{ (For instability)} \tag{10}$$

Clearly, the fluid damping C_{xx}, if positive, reinforces the other machine damping C_0, and promotes stability, whereas the cross-coupled stiffness K_{xy} is equivalent to a negative damping $-K_{xy}/\Omega_0$. The cross-damping C_{xy} is seen to have relatively minor effect on the dynamics, since, as K_{xx}, it only affects the natural frequency, and not the growth or decay rate. In some instances, the fluid-related stiffness is not negligible, and can be exploited to help relocate the critical frequencies away from unfavorable ranges. This was, in fact, the approach taken in the SSME redesign [52]. The two principal avenues for improving rotordynamic stability-increasing damping or raising the natural frequency are both exemplified on the right-hand side of Eq. (10).

4. Some Examples of Cross-Coupled Force Generation

Among the mechanisms which have been identified as contributors to the production of destabilizing cross-forces are (a) Pressure non-uniformity in labyrinth and other seals; (b) Non-uniform driving force in turbines due to tip leakage effects [59, 60]; (c) Non uniform pressure and driving force in pump impellers, also related to leakage effects [55, 56]. Other effects are reviewed in Ref [57]. Rather than attempting here a general coverage of this rather rich field, we will only explain in some detail the labyrinth seal and blade–tip effects, which, aside from their importance in practical cases, can be seen as prototypes of the relevant physics.

(a) Labyrinth Seals. The existence of flow swirl at the entrance to an offset labyrinth seal (and, in modified form, to other seals as well) gives rise to a rotation of the pressure pattern produced by the offset, and hence produces cross-coupled forces. Two principal effects can be identified here [58]. One of these can be described as follows: the fluid in the gland of the seal (a single-cavity labyrinth, for simplicity) circulates azimuthally in the varying area created by the shaft offset (Fig. 3).

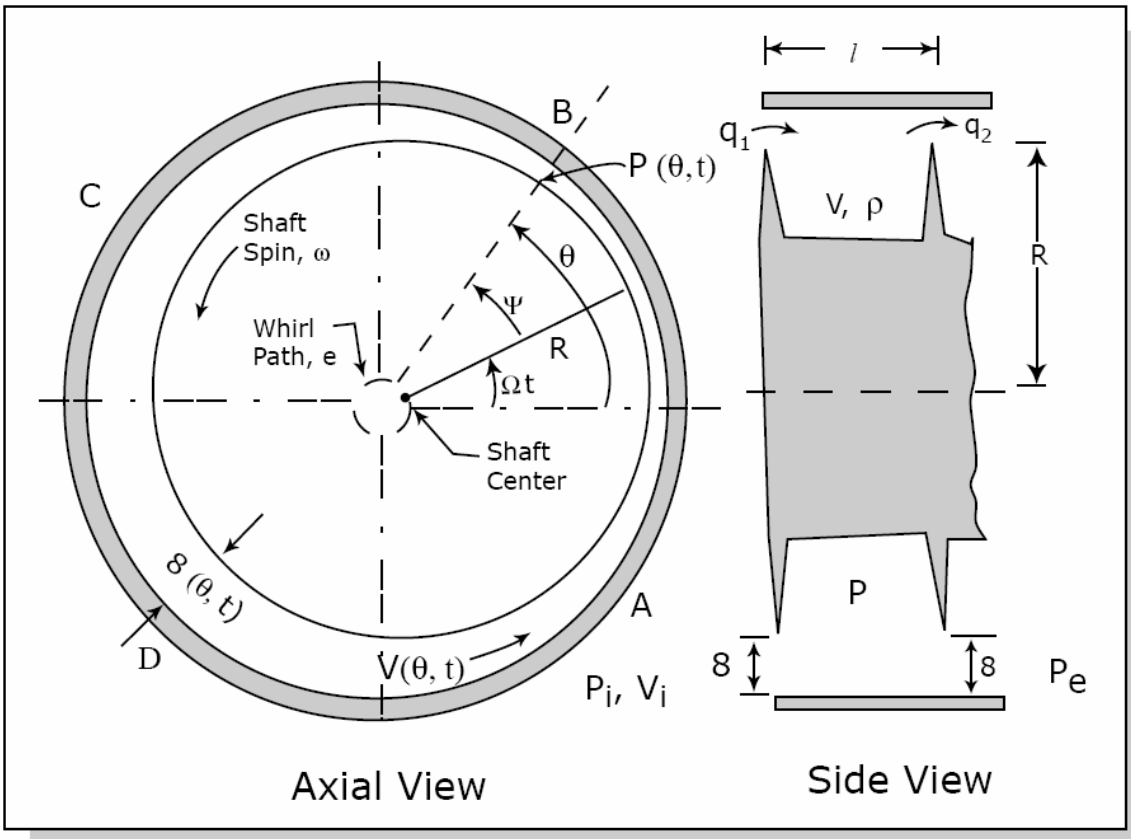

Fig. 3: Kinematic quantities associated with a labyrinth seal. The shaft is spinning at an angular frequency ω, while simultaneously undergoing a circular precession of amplitude *e* and frequency Ω.

If the tangential velocity V were constant (which is approximately true under some conditions), the circulating flux $\rho V l (h+\delta)$ would need to be increasing with ϑ at points where the depth $(h+\delta)$ (h= sealing strip height, $\delta(\vartheta)$ = local gap) is increasing. This implies an excess of leakage from upstream of the seal into the cavity over that from the cavity to downstream of it, which is accomplished by a locally depressed $P(\vartheta)$. Thus, the pressure would be minimum at point C in Fig. 3. and maximum at point A. The net integrated pressure force is then rotated 90° from the shaft displacement in the direction of the swirl. Since the pressure pattern is anchored to the whirling gap pattern, it is clear that, for a given inlet swirl, the effect will depend on the whirling speed Ω and will, in fact, be zero when $\Omega R = \overline{V}$, because the gland fluid will then not move tangentially with respect to the whirling gap pattern. This argument is modified by the azimuthal variations induced on the velocity V, which were so far neglected. A more complete analysis [58] gives the force components parallel and perpendicular to the displacement as

$$F_{\parallel} = \frac{\pi}{4}\left(\frac{lh}{R\bar{\delta}}\right)\left(l^2\Delta P\right)\frac{e/\delta}{1+f^2} \qquad ; \quad f = \left(\frac{lh}{R\bar{\delta}}\right)\frac{\sqrt{\Delta P/\rho}}{\overline{V-\Omega R}} \tag{11}$$

$$F_{\perp} = \frac{\pi}{2} l^2 \sqrt{\rho\Delta P}\left(\overline{V}-\Omega R\right)\frac{e/\delta}{1+f^2} \tag{12}$$

where $\Delta P = P_i - P_e$, and we have assumed incompressible, inviscid fluid and a circular whirling motion about the casing center with amplitude e. Aside from a negative K_{xx} (in the notation of (Eq. 1), we see from (12) that positive K_{xy} and C_{xx} are predicted. The presence of higher order terms in Ω in Eq. 12 also indicated effective mass and other effects, but these have little dynamic impact. The main factors are related in this case through

$$C_{xx} = \frac{R}{\overline{V}}\,K_{xy} \tag{13}$$

and the simple case in which velocity variations are neglected is recovered when

$$\frac{lh}{R\bar{\delta}} \ll 1 \quad \text{in Eqs. (11) and (12)}$$

The second seal mechanism depends on the existence of friction between the circulating fluid and the rotor and casing surfaces (although the resultant cross-force is still a pressure, and not a frictional force). Because of friction, the mean tangential velocity $\overline{V}$ is usually slightly less than the inlet tangential velocity $\overline{V}_i$ and leakage fluid entering the gland from upstream will continuously add tangential momentum

to the gland fluid as they mix, in a manner similar to the operation of an ejector pump. This effect is strongest at point D (Fig. 3), where the gap is widest, and weakest at point B. Thus, a positive pressure gradient $\frac{\partial P}{\partial \vartheta}$ will exist at D, and a negative one at B, again leading to a pressure maximum at A and to a cross-force along the perpendicular axis$(\perp)$. Since this effect does not depend on fluid velocities relative to the whirling frame, it does not show whirl velocity dependence, and does not contribute to damping(C_{xx}). A simplified analysis, neglecting tangential velocity variations, gives for this effect

$$F_{\parallel} = \pi R^2 \left(\frac{R\delta}{hl}\right) \frac{\rho\left(V_i - \overline{V}\right)^2}{1+g^2} \frac{e}{h} \qquad (14)$$

$$F_{\perp} = \pi R^2 \frac{\sqrt{\rho \Delta P}\left(V_i - \overline{V}\right)}{1+g^2} \frac{e}{h} \quad ; \quad g = \frac{R\delta}{hl} \frac{V_i - \overline{V}}{\sqrt{\Delta P/\rho}} \qquad (15)$$

Because of the importance of inlet swirl in promoting seal cross-forces, de-swirling fins can be used ahead of the seal, if this is at all practical. Experiments [58] have validated the above cross-force mechanisms, while also pointing out the importance of other secondary effects, particularly for direct stiffness.

Both force components are greatly magnified in smooth seals with very small clearance [52, 61]. Whether the added cross-coupling or the added stiffness is more important when one of these is substituted for a labyrinth, must be directly assessed through dynamic analysis for each specific case.

(b) Turbine Blade-Tip Effects. It was independently pointed by Alford [62] and Thomas [63] that the sensitivity of blade-tip losses to blade-tip gap in turbines should produce forward-whirling cross forces. The basic mechanism is simple: When the turbine rotor is offset from its center, the blades on the side where the tip gap is reduced will gain efficiency, and hence produce more tangential driving force than average, and the opposite will happen on the side where gap opens up. Integrating these forces around the periphery yields, in addition to the desired torque, a side force in the forward-whirling direction (see Fig. 4). It is easy to translate this argument into an explicit equation for the cross-force. Let $\beta = \frac{-\partial \eta}{\partial(\delta / H)}$ be the sensitivity of blade efficiency to relative tip clearance δ / H, where δ is the clearance and H is the blade height. This factor is of the order of 1-5, depending on design and operating point.

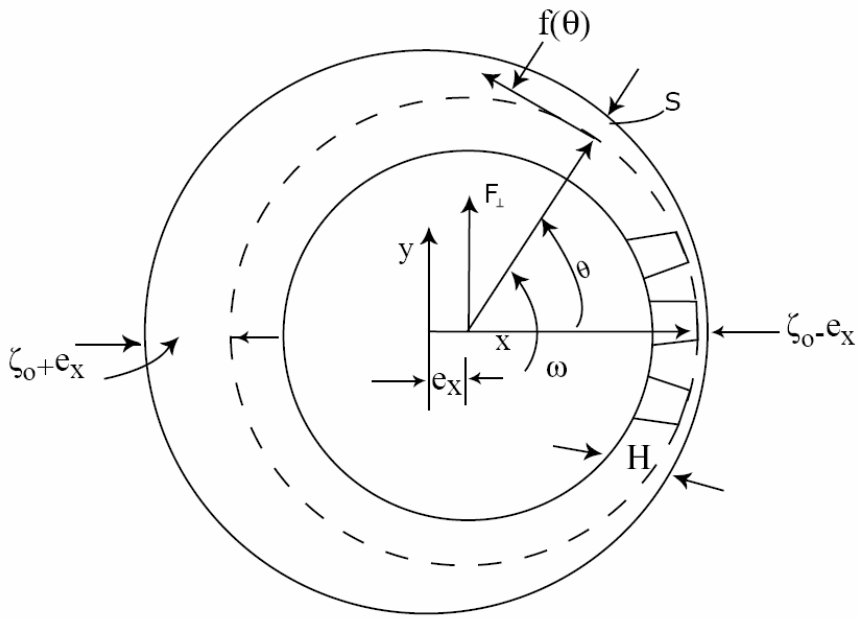

Fig. 4. Geometry of Alford's Model

The tangential force *f* per unit length along the perimeter is then approximated as

$$f \cong \bar{f} - \beta\left(\frac{\delta - \bar{\delta}}{H}\right) \tag{16}$$

although it must be pointed out that this equates work loss to efficiency loss, and hence it ignores pressure ratio variations also induced by the offset. The clearance perturbation $\delta - \bar{\delta}$ varies in proportion to the offset *e*, and sinusoidally with azimuth ϑ , and so, upon projection in the direction perpendicular to the offset, and integration, one obtains

$$F_{\perp} = \pi R \bar{f} \beta \frac{e}{H} = \beta \frac{Q}{2R} \frac{e}{H} \tag{17}$$

where $Q = 2\pi R \bar{f}$ is the turbine torque. The direct force $F_{\parallel}$ is predicted to the zero.

The existence of these forces was confirmed experimentally in Ref. [64] and, in more detail, in Refs [59,60] where it was found that, in addition to the above mechanism, a second source of cross-forces is a tangentially rotated pressure nonuniformity is acting on the turbine hub. The contribution of this component is additive to the basic Alford/Thomas effect, and amounts typically to 40% of the total cross-force. In addition, both mechanisms also give stiffening force components (along with offset direction).

One important question which remains experimentally unanswered is whether or not the Alford/Thomas forces show a significantly sensitivity to whirl speed, i.e., whether they provide C_{xx} component for the stiffness matrix. The original argument would predict no such sensitivity. A fairly obvious extension, accounting for change $\Omega e \cos\vartheta$ to the basic blade speed ωR can be shown to yield a modified Alford factor

$$\beta' = \beta - \frac{1}{\psi}\frac{H}{R}\frac{\Omega}{\omega} \tag{18}$$

where $\psi = Q\omega / \dot{m}(\omega R)^2$ is the turbine work coefficient, which is close to 2 for impulse turbines. Since $H/R \sim 0.2$ and Ω/ω (whirl to spin ratio) is ~ 0.5, we see that $\beta' \approx \beta - 0.05$, which would not be significant. Other velocity-dependent effects may arise form time lags in the azimuthal redistribution of flow approaching a whirling rotor; these would also be of order H/R, but no direct experimental evidence exists for their magnitude. Ref [60] does provide a theoretical model for this effect however the Alford-Thomas forces can be very large, requiring damping log decrements of the order of 0.1 in typical rocket turbopumps.

References Cited

48. F. Ferlitia et al. "*Rotor Support for the STME Oxygen Turbopump*". Paper AIAA 92-3282. 28th Joint Propulsion Conference, July 1992.

49. J.P. Den Hartog, Mechanical Vibration, McGraw-Hill book Company, 1956.

50. Childs, Dara W. Turbomachine Rotor Dynamics: Phenomena, Modeling and Analysis, Wiley Interscience, N.York, 1993.

51. J.M. Vance, Rotordynamics of Turbomachinery, Wiley, New York, 1988.

52. M.C. Ek "*Solution of the Subsynchronous Whirl Problem in the High-Pressure Hydrogen Turbomachinery of the Space Shuttle Main Engine*". J. of Spacecraft, Vol. 17, No. 3.

53. G.R. Mueller, "*Finite Elements Models of the Space Shuttle Main Engine*" NASA TM-78260, Jan. 1980.

54. F. Ehrich "*The Role of Bearing Support Stiffness Anistropy In Suppression of Rotordynamic Instabilities*". ASME 12th Biennial Conf. on Vibration and Noise. Montreal, Canada, Sept. 1989.

55. Jery, B. Acosta, A. J., Brennen, C.E. and Caughey, T.K. " *Hydrodynamic Impeller Stiffness, Damping and Inertia in the Rotordynamics of Centrifugal Flow Pumps*". NASA CP-2338, 1984, pp.137-160.

56. Chamie, D.S., Acosta, A.J., Brennen, C.E. and Caughey, T.K. "*Experimental Measurements of Hydronamic Radial Forces Stiffness Matrices for a Centrifugal Pump Impeller*", ASME JI. Of Fluids Engineering, Vol.107, No. 3, 1985, pp 307-315.

57. F. Ehrich and D.W Childs, "*Self-Excited Vibrations in High Performance Turbomachinery*", Mech. Engineering, ay 1984.

58. Knox T. Millsaps, "*The impact of Unsteady Swirling Flow in a Single-Gland Labyrinth Seal on Rotordynmics Stability: Theory and Experiment*". Ph.D. Thesis, MIT, 1992.

59. M. Martinez –Sandues, B. Jaroux, S.J. Song and S. Yoo "Measurement of Turbines Blade-Tip Rotor dynamic Excitation Forces" J. of Turbomachinery, 117, 3, July 1995, pp. 384-393.

60. S.J. Srig and M. Matrinz-Sanchur, "Rotordyanamic Effects due to Turbine-Tip Leakage: Part I, Black-Scale Effects. Part II, Radius Scale Effects and Experimental Verification ". J. of Turbomachinery, 119, 4, Oct 1997, pp. 695-714.

61. D.W. Childs, "*Dynamic Analysis of Turbulent Annular Selas Based on Hir's Lubrication Equation*" ASME J. of Lubrication Technology, V.105, No. 3, 1983, pp. 437-445.

62. J.S. Alford, "*Protesting Turbomachinery from Self-Excited Rotor Whirl*", J. of Engineering for Power, Oct. 1965.

63. H.J. Thomas "*Unstable Oscillations of turbine Rotors Due to Steam Leakage in* the Clearance Of the sealing Glands and the Buckets". Bull. Scientifique A.J.M., Vol. 71, 1958, pp 1039-1063.

64. K. Urlicks, "*Clearance Flow Generated Transverse Forces at the Rotors of Thermal Turbomachines*". NASA TM -77292, Oct.1983. (Translated from Doctoral Dissertation at the Technical Univ. of Munich, 1975).